ChemPubSoc Europe

DOI: 10.1002/chem.201600286

CHEMISTRY A European Journal Full Paper

Copper-Chelating Tripeptides

Histidine-Rich Oligopeptides To Lessen Copper-Mediated Amyloid-β Toxicity

Ana B. Caballero,*[a] Laia Terol-Ordaz,[a] Alba Espargaró,[b] Guillem Vázquez,[a] Ernesto Nicolás,[a] Raimon Sabaté,[b] and Patrick Gamez*[a, c]

Abstract: Brain copper imbalance plays an important role in amyloid-β aggregation, tau hyperphosphorylation, and neurotoxicity observed in Alzheimer's disease (AD). Therefore, the administration of biocompatible metal-binding agents may offer a potential therapeutic solution to target mislocalized copper ions and restore metallostasis. Histidine-containing peptides and proteins are excellent metal binders and are found in many natural systems. The design of short peptides showing optimal binding properties represents a promising approach to capture and redistribute mislocalized metal ions, mainly due to their biocompatibility, ease of synthesis, and the possibility of fine-tuning their metal-binding affinities in order to suppress unwanted competitive binding with copper-containing proteins. In the present study, three peptides, namely **HWH**, **HK^{C}H**, and **HAH**, have been designed with the objective of reducing copper toxicity in AD. These tripeptides form highly stable albumin-like complexes, showing higher affinity for Cu^{II} than that of Aβ(1-40). Furthermore, **HWH**, **HK^{C}H**, and **HAH** act as very efficient inhibitors of copper-mediated reactive oxygen species (ROS) generation and prevent the copper-induced overproduction of toxic oligomers in the initial steps of amyloid aggregation in the presence of Cu^{II} ions. These tripeptides, and more generally small peptides including the sequence His-Xaa-His at the N-terminus, may therefore be considered as promising motifs for the future development of new and efficient anti-Alzheimer drugs.

Recent years have witnessed increasing evidence on the relationship between copper dyshomeostasis, among other metal ions such as iron and zinc, and the advent of neurodegenerative disorders such as Alzheimer's disease (AD).[1,2] Copper can bind to amyloid beta-protein (Aβ) and modulate its aggregation mechanism, and indeed Aβ aggregates represent one of the hallmarks of AD.[3] The binding of copper ions to the protein promotes the generation of soluble oligomeric species, which are believed to be the most toxic form of Aβ.[4] Actually, such Aβ-copper complexes can catalyze the production of reactive oxygen species (ROS) through Cu^{II}/Cu^{I} redox cycling in the presence of natural reducing agents such as ascorbate,[5] ultimately leading to oxidative stress, which is another critical early event in AD.

[a] *Dr. A. B. Caballero, L. Terol-Ordaz, G. Vázquez, Dr. E. Nicolás, Prof. P. Gamez*
Department of Inorganic and Organic Chemistry
University of Barcelona, Martí i Franquès 1–11, 08028 Barcelona (Spain)
E-mail: ana.caballero@ub.edu
patrick.gamez@qi.ub.es

[b] *Dr. A. Espargaró, Dr. R. Sabaté*
Department of Physical Chemistry, Faculty of Pharmacy and
Institute of Nanoscience and Nanotechnology (IN_2UB)
University of Barcelona, Avda. Joan XXIII 27-31, 08028 Barcelona (Spain)

[c] *Prof. P. Gamez*
Institució Catalana de Recerca i Estudis Avançats (ICREA)
Passeig Lluís Companys 23, 08010 Barcelona (Spain)

Supporting information for this article and ORICDs for some of the authors are available on the WWW under http://dx.doi.org/10.1002/chem.201600286.

Therefore, copper chelation can be considered as a valuable therapeutic strategy to capture misplaced copper ions and to suppress their potential redox activity (to reduce oxidative stress). In this context, small peptide-based chelators may represent molecules of choice, owing to their biocompatibility and potentially adjustable metal-binding properties. Indeed, the incorporation of histidine residues (His) in a peptidic chain will lead to extremely efficient copper ligands, the metal-binding properties of which can be modulated by varying the number of these amino acids (AAs) and their position(s) in the sequence.[6]

Our current research interests are focussed on the design of potential copper-binding oligopeptides, for instance of the type His-Xaa-His (where Xaa denotes any AA other than His), deprotected at both ends. This sequence is frequently encountered in biomolecules; for example, it is observed as His-Thr-His in peptidylglycine α-hydroxylating monooxygenase[7] and dopamine β-monooxygenase,[8] as His-Val-His in Cu, Zn-superoxide dismutase SOD5[9] and particulate methane monooxygenase,[10] and as His-Gln-His in amyloid-like protein 2 (APLP2).[11] Moreover, four highly conserved His-Xaa-His motifs are found in the catalytic centers of some copper-containing oxidases (i.e., ascorbate oxidase, fungal laccase, and ceruloplasmin).[12] A pentapeptide domain with the sequence His-Leu-His-Trp-His is present in the amyloid precursor protein (APP) associated with the development of Alzheimer's disease.[13] However, it should be mentioned that these sequences are all inserted within larger proteins, and therefore do not exhibit an N-terminal his-

tidine moiety, in contrast to our His-Xaa-His tripeptides, which may therefore form an amino terminal Cu^{II}- and Ni^{II}-binding (ATCUN) motif upon binding to copper.

Copper chelation by naturally occurring or (bio-inspired) synthetic peptides has been described, for example by the Gly-His-Lys tripeptide first isolated from human plasma,[14] the N-terminal metal-binding sequence Asp-Ala-His-Lys of human albumin,[15,16] and some H2A-histone model hexapeptides.[17] Recently, Mital et al. have demonstrated that N-truncated Aβ(4-42), which is a dominant Aβ isoform that is even found in healthy brains, exhibits an N-terminal Phe-Arg-His sequence that binds copper(II) ions with an affinity three orders of magnitude higher than that of Aβ(1-42); hence, the Aβ(4-42) fragment may play a role in the metal homeostasis of the central nervous system.[18]

In the present study, the copper(II)-binding properties under physiological conditions of three His-Xaa-His tripeptides, with Xaa = Trp, N^{ε}-coumarin-labeled Lys, or Ala (**HWH**, **HK^{C}H**, and **HAH**, respectively; see Figure 1), have been investigated. This length of peptide, namely three AAs, was chosen because it is believed to be appropriate for an efficient metal wrap. The co-

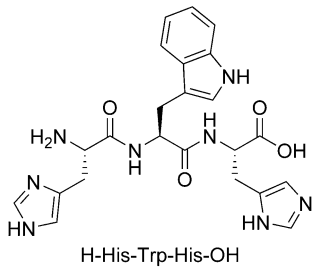

H-His-Trp-His-OH

(**HWH**)

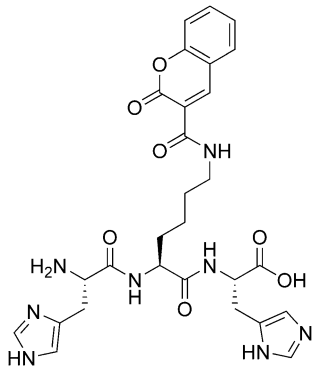

H-His-Lys(coumarin)-His-OH

(**HK^{C}H**)

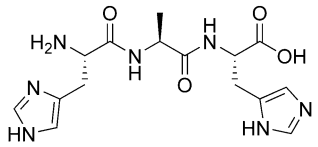

H-His-Ala-His-OH

(**HAH**)

Figure 1. Structures of the copper-chelating tripeptides investigated, that is, L-histidyl-L-trytophanyl-L-histidine (**HWH**), L-hystidyl-(N^{ε}-coumarin-3-ylcarbonyl)-L-lysyl-L-histidine (**HK^{c}H**), and L-histidyl-L-alanyl-L-histidine (**HAH**).

existence of a free N-terminal amino group and a histidine residue at the third position (Figure 1) was envisaged as favoring the formation of a highly stable, albumin-like coordination species at physiological pH, and the histidine at position one was expected to enhance the binding affinity kinetically (as shown in the section "Determination of the Conditional Binding Constants by Fluorescence Spectroscopy" below; replacement of His1 by glycine leads to a distinctly lower copper-binding affinity of the resulting **GWH** compared to that of **HWH**). Finally, specific central AAs were selected; one natural, that is, tryptophan (**W**), and one synthetic, that is, N^{ε}-(coumarin-3-ylcarbonyl)lysine (**K^{C}**). Fluorescent AAs were chosen to label the corresponding tripeptides, allowing both fluorescence studies and their detection (which may be very useful for in vivo studies). The central AA of the third tripeptide, namely a simple alanine (**A**) residue, was selected for comparison purposes (as a non-fluorescent reference peptide).

The binding modes of these three peptides to copper(II) ions and their efficiencies (i.e., binding affinities) were first investigated. Subsequently, in vitro studies, including competitive binding experiments with Aβ and inhibition studies of copper-catalyzed ROS production, were carried out. Lastly, their effects on the copper-mediated process of Aβ aggregation were examined. Given that Aβ(1-42) formed by bacterial inclusion bodies (IBs) displays similar structural properties to those of pathological amyloid fibrils,[19] and that these structural properties are not affected when Aβ(1-42) is attached to aggregation reporters such as the green fluorescent protein (GFP),[20] GFP-Aβ(1-42) fusion constructs were used to demonstrate the preferential copper(II) binding of the tripeptides. Furthermore, the in vitro time courses of Aβ(1-40) aggregation in the presence and absence of copper(II) ions, and of **HAH**, **HK^{C}H**, or **HWH**, have been examined.

Results and Discussion

Copper-binding studies: The aggregation of amyloid-type proteins can be investigated by UV/Vis spectrophotometry, measuring the absorbance/turbidity (resulting from precipitation) at $\lambda = 405$ nm in a buffered solution (HEPES, pH 7.4).[21] We have used this procedure to study the binding of copper(II) ions to the His-Xaa-His tripeptides, since we observed that an increase in the copper concentration (with respect to the peptide concentration) led to the precipitation of copper/peptide species. The absorbance changes obtained upon the addition of increasing amounts of Cu^{II} ions to **HWH**, **HK^{C}H**, and **HAH** are depicted in Figure 2a. Clearly, the reaction mixtures did not absorb at 405 nm until a 1:1 ratio of copper/tripeptide was reached, whereupon an increase in the absorbance was detected (Figure 2a). Subsequently, analogous experiments were carried out following the absorption band corresponding to d-d transitions. Indeed, the copper/peptide complexes exhibited an absorption band at $\lambda = 515$ nm ($\varepsilon = 105\ M^{-1}cm^{-1}$) for **HWH**, $\lambda = 515$ nm ($\varepsilon = 94\ M^{-1}cm^{-1}$) for **HK^{C}H**, and $\lambda = 520$ nm ($\varepsilon = 113\ M^{-1}cm^{-1}$) for **HAH** (Figure S1). In this case as well, a change in absorbance was observed above a 1:1 copper/tripeptide ratio (Figure 2b). Therefore, these studies suggested

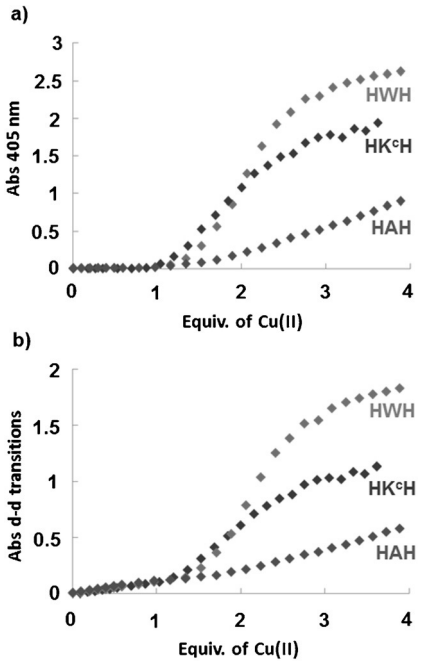

Figure 2. Determination of the stoichiometries of the Cu^{II}/peptide complexes for **HAH**, **HWH**, and **HK^{C}H** by monitoring the complex formation and precipitation through a) the absorbance/turbidity (resulting from precipitation) at 405 nm, and b) the absorbance ($\lambda = 515$ nm for **HK^{C}H** and **HWH** and $\lambda = 520$ nm for **HAH**) corresponding to copper(II) d-d transitions.

a 1:1 binding stoichiometry. This was further confirmed by ESI-MS analyses, which showed the sole formation of a [copper-peptide] species, even in the presence of two equivalents of the metal ion (Figures S2–S4).

The relatively low λ values of the d-d transitions (see above) suggest that strong-field ligands are coordinated to the metal center, such as deprotonated peptidic nitrogen atoms.[22] According to the empirical equation described by Sigel and Martin for square-planar copper(II) complexes,[23] the observed $\lambda^{d-d}{}_{max}$ values are consistent with the presence of four nitrogen atoms in the equatorial plane;[24] the predicted value for an {NH_2, N^-, N^-, N_{im}} coordination environment is around 530 nm.[25] Thus, a number of copper peptidic complexes exhibiting this coordination environment have been reported, which show $\lambda^{d-d}{}_{max}$ values in the range 510–530 nm.[25,26] This binding mode, also known as the amino terminal Cu^{II}- and Ni^{II}-binding motif (ATCUN), is found in a wide range of natural metal-containing proteins, the best known example being human serum albumin.[27]

The circular dichroism (CD) spectra of buffered solutions (HEPES, pH 7.4) of the different peptides with added copper display a broad band centered at $\lambda = 321$ (**HWH**), 338 (**HK^{C}H**), and 310 nm (**HAH**) (Figure 3), characteristic of a ligand-to-metal charge-transfer transition involving a deprotonated amide donor.[28] This band most likely also includes the $N_{imidazole}$-Cu^{II} charge-transfer transition;[29] indeed, shoulders are observed at around 350 nm (for **HWH** and **HAH**, Figure 3), which are clearly due to the $N_{im} \rightarrow Cu^{II}$ charge-transfer transition.[30] More intense bands appear at 265 nm for **HWH** and **HAH** and at 288 nm for **HK^{C}H** (Figure 3), which can be ascribed

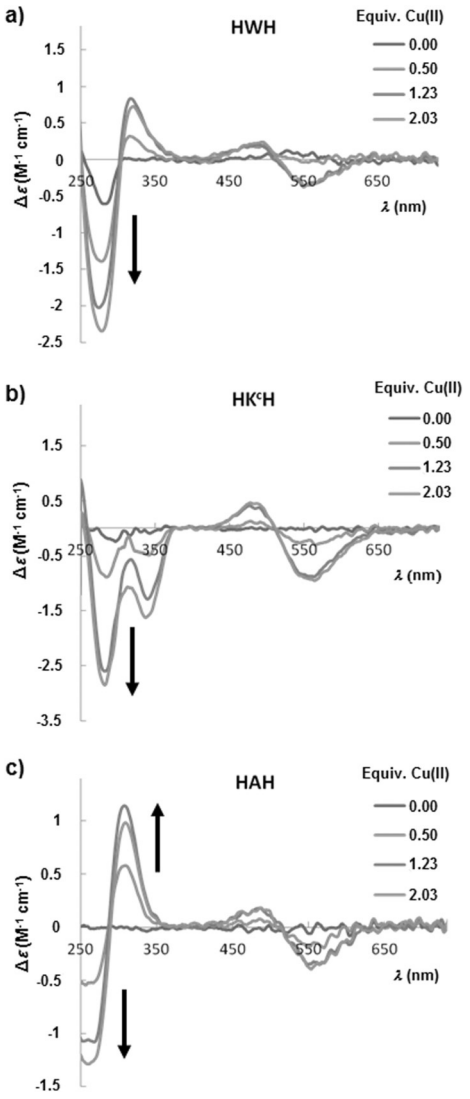

Figure 3. Circular dichroism spectra of a) **HWH**, b) **HK^{C}H**, and c) **HAH** upon addition of increasing amounts of copper(II) chloride.

to both intraligand imidazole and $N_{amine} \rightarrow Cu^{II}$ charge-transfer transitions.[31,32] The two d-d bands (Cotton effect) significantly below 600 nm (i.e., at high energies), specifically at around 560 and 485 nm for all peptide/Cu complexes (Figure 3), also point to the formation of 4N species involving deprotonated amide ligands.[31]

In summary, the UV/Vis and CD spectroscopic data suggest a coordination environment analogous to that found for copper bound to albumin. It should also be noted that peptide-to-copper ratios of 1:2 and 2:1 did not show any shift of the d-d band (i.e., from that observed for the 1:1 complex), corroborating that solely the 1:1 species is formed.

^{1}H and ^{13}C NMR studies: The paramagnetism of copper(II) was used to further investigate its interaction with the tripeptides, taking advantage of the severe broadening of the NMR signals upon copper binding.[33] The ^{1}H and ^{13}C NMR spectra for **HWH**, **HK^{C}H**, and **HAH** in the presence of 0.01 equiv of copper(II) are shown in the Supporting Information (Figures S5–S10). Since comparable peak-broadening effects were observed

for the three peptides, a single figure is presented to describe the relative intensities of the copper-induced signal alterations, in which a gray color gradient is used to characterize the magnitude of the peak broadening/alteration (Figure 4).

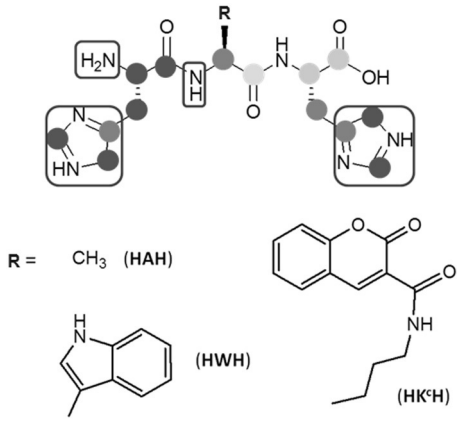

Figure 4. Schematic representation of the magnitude of ^{13}C NMR peak broadening upon addition of 0.01 equiv of copper(II) to the different peptides in D_2O at pH 7.4. Dark dots symbolize strongly affected signals while light dots indicate less affected signals. The binding moieties deduced from these studies are shown in squares.

The effect of copper on the ^{1}H and ^{13}C NMR signals is manifested in a decrease in their intensity due to broadening. As indicated in Figure 4, the positions that are most affected by the paramagnetic metal ion are those that are close to binding moieties, namely the N-terminal amino group, the first amide function, and the two imidazole rings (the dark dots in Figure 4). These features are at variance with the ATCUN motif proposed above, in which only one of the histidine residues (i.e., that at position three) coordinates to copper. In addition, these NMR data apparently rule out metal-binding by the second amide function. The significant alteration of the signals of the first His residue may be justified either by the proximity (viz. not through direct binding) of the metal ion or by a fast intramolecular exchange between one histidine site and the other. However, such His1 vs His3 exchange cannot explain the non-involvement of the second amide function (see the light dots in Figure 4).

The very marked broadening of the ^{1}H signals for all of the investigated peptides, following the addition of only 1% copper, is indicative of a fast copper(II) exchange (at least faster than the millisecond time-scale of NMR). These observations are in marked contrast to previous studies with histidine-containing peptides, whereby 10 mol% or even higher amounts of copper were needed to produce significant changes in line widths or/and chemical shifts of the peptidic signals.[16,34] In the present case, the use of 0.1 equiv of copper(II) with **HAH** was sufficient to observe extremely broadened ^{1}H signals (Figure S11) and the disappearance of the signals in the ^{13}C spectrum.

EPR studies: EPR spectroscopy was used to investigate the coordination environment of the copper(II) ions, with the objective of clarifying the observed inconsistency between the UV/Vis/CD data and the NMR results. The EPR spectra of frozen solutions of the three copper/tripeptide complexes (obtained by mixing a 10% excess of the peptidic ligand with respect to the metal salt) are comparable (Figure 5 and Figure S12); axial symmetry is indicated by the components of the g tensor, with $g_{\parallel} > g_{\perp} > g_e$.[35] These data may characterize a square-planar, square-pyramidal, or axially elongated tetragonal octahedral

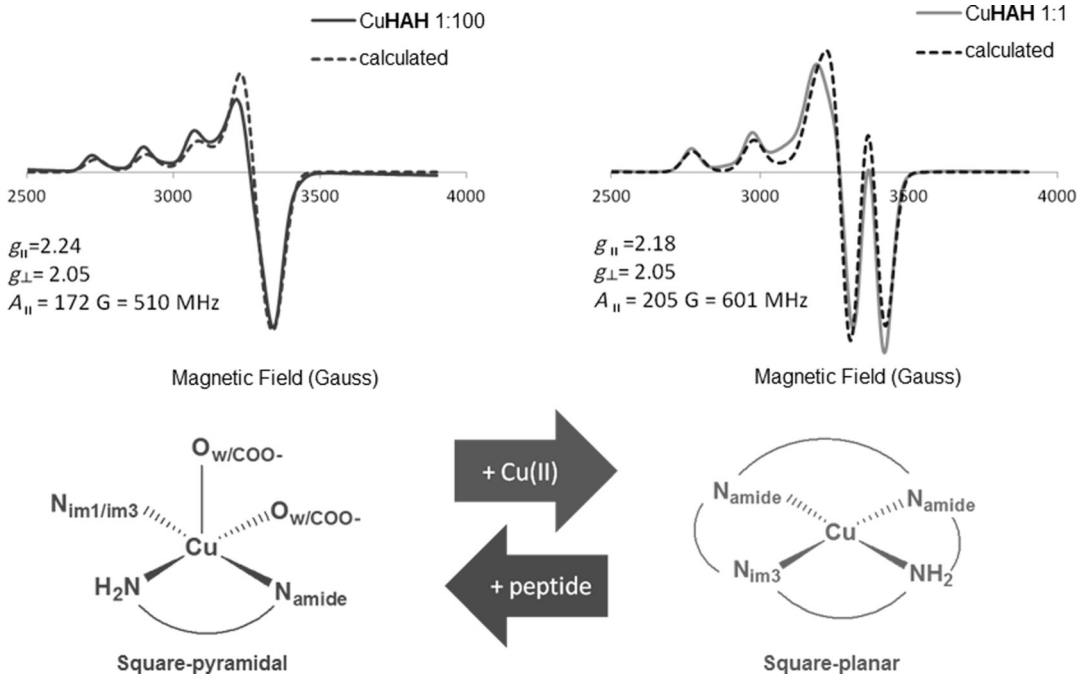

Figure 5. EPR spectra of 1:1 and 1:100 Cu^{II}-**HAH** solutions recorded at 77 K, and proposed coordination environments and geometries for the corresponding species.

geometry. Actually, the $g_{\parallel}$, $g_{\perp}$, and $A_{\parallel}$ values of 2.18, 2.05, and 601 MHz (205 G), respectively, are consistent with a 4N complex exhibiting a square-planar geometry of albumin type.[36]

Next, EPR experiments were carried out using the conditions applied for the NMR studies, namely a peptide-to-copper ratio of 100:1 (see above). Remarkably, the corresponding EPR data were found to be completely different to those obtained when using (nearly) equimolar amounts of Cu^{II} ions and peptide (Figure 5). The $g_{\parallel}$ value increased to 2.24 while the hyperfine parallel constant $A_{\parallel}$ decreased significantly to 510 MHz (172 G). The increase in $g_{\parallel}$ is indicative of an increase in the electron-withdrawing character of the ligands, which, together with the marked decrease in $A_{\parallel}$, suggests the replacement of one or two nitrogen atoms by oxygen atoms.[37] Unfortunately, the lack of resolution of the superhyperfine structure does not allow us to determine with better accuracy the number of nitrogen atoms bound to the copper ion in the equatorial plane.

As mentioned above, the NMR experiments suggested that the two imidazole rings coordinate to the metal center, in addition to the N-terminal amine and the first amide group of each tripeptide. In the pH range 4–6, the very efficient histamine-like binding mode $\{NH_2, N_{im}\}$ is most likely predominant, impeding amide deprotonation.[6,38] At higher pH values, for instance at pH 7.4, deprotonation of the first amide function can occur, and the resulting N_{amide}^- can replace the His1 ligand, generating a CuN_3O-type species with an $\{NH_2, N^-, N_{im}, O_w/O_{carbox}\}$ donor set or a square-pyramidal CuN_3O_2 species with an O_w/O_{carbox} atom at the apical position. In these two possible species, the imidazole moiety may belong to the His3 residue of the coordinated peptide or a histidine residue (either His1 or His3) of a second peptide. In fact, interaction with a second tripeptide would be expected to occur at such a high ligand excess (i.e., ligand:copper = 100:1). Hence, intermolecular binding of a histidine residue will be favored by deprotonation of the second amide group at pH 7.4, which may be triggered upon intramolecular His3 binding, thereby generating the extremely stable albumin-like coordination moiety. The EPR data are typical of a square-pyramidal geometry and are consistent with a CuN_3O_2 species in which one oxygen atom binds at the apical position. Considering all of the above observations, an $\{NH_2, N^-, N_{im(His1/3)}, O_w/O_{carbox}, O_w/O_{carbox}\}$ donor set can be proposed for a 100:1 peptide:copper mixture.

Determination of the conditional binding constants by fluorescence spectroscopy: Intrinsic fluorescence measurements were performed with the emitting tripeptides **HWH** and **HK^{C}H** to determine the apparent and conditional affinity constants of their copper(II) complexes. As expected, emission quenching by the copper(II) ions was observed, with a better efficiency for **HWH** than for **HK^{C}H**. Stern–Volmer plots were obtained at pH 7.4, which exhibited an upward curvature (data not shown), indicating the simultaneous operation of dynamic and static quenching processes.[39]

Upon addition of up to 0.5 equiv of copper(II) ions, the fluorescence data could be fitted to the simple and well-known Stern–Volmer equation,[40] giving K_{sv} values of 1.7×10^5 and $1.3\times10^5\ M^{-1}$ for **HWH** and **HK^{C}H**, respectively (with $r^2 > 0.99$). In the case of **HWH**, complete quenching of the fluorescence was observed with an equimolar amount of copper, whereas 12% of the coumarin emission remained with **HK^{C}H**. The latter observation may be explained by the greater distance between the fluorescent group and the copper-binding site in tripeptide **HK^{C}H**.

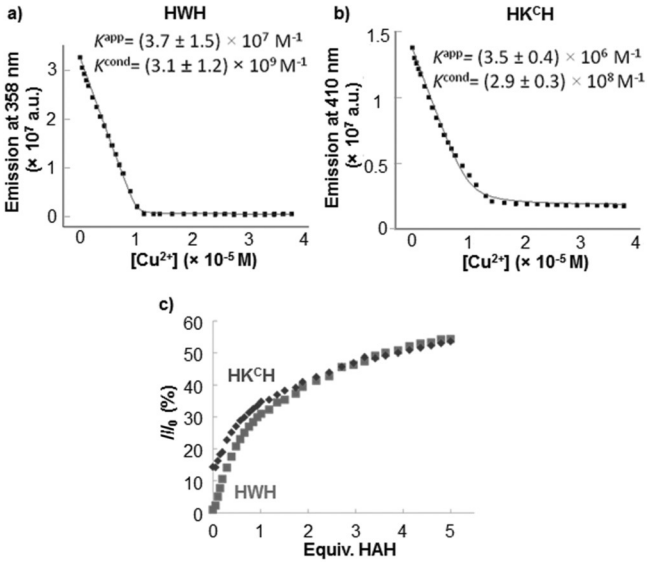

Figure 6. Fitting of the fluorescence titration data to Eq. (2) and conditional affinity constants obtained for a) **HWH** and b) **HK^{C}H**. c) Plot illustrating the strong but partial recovery of the emissions of **HWH** and **HK^{C}H** upon addition of **HAH**. [Peptide] = 10 μM in HEPES (100 mM, pH 7.4).

To determine the apparent binding constants (K^{app}), the experimental data were fitted to Equation (1),[41,42] and the corresponding plots are shown in Figure 6 a,b (see Experimental Section for details).

$$I = I_0 + \frac{I_{lim} - I_0}{2[L]}\left([L] + [Cu^{2+}] + \frac{1}{K^{app}} - \sqrt{\left([L] + [Cu^{2+}] + \frac{1}{K^{app}}\right)^2 - 4[L][Cu^{2+}]}\right) \quad (1)$$

where [L] and $[Cu^{2+}]$ are the total concentrations of the peptide and copper(II) ions, respectively, K^{app} is the apparent affinity constant of the Cu^{II}-peptide complex, and I_0 and I_{lim} denote the fluorescence intensities of the free and the fully complexed peptide, respectively. The determination coefficients (r^2) were in all cases > 0.99.

The corresponding K^{app} values were evaluated as $3.7\times10^7\ M^{-1}$ ($r^2 > 0.99$) for **HWH** and $3.5\times10^6\ M^{-1}$ ($r^2 > 0.99$) for **HK^{C}H**. Considering the binding affinity of the buffer, namely HEPES (used in high excess), the K^{app} constants were corrected by applying Equation (2);[43] subsequent conditional binding constants (K^{cond}) of 3.1×10^9 and $2.9\times10^8\ M^{-1}$ were evaluated for **HWH** and **HK^{C}H**, respectively (see the Experimental Section for details).

$$\log K^{cond} = \log K^{app} + \log\left(1 + \beta_{Cu-buffer} x \frac{[buffer]}{1 + 10^{-pH+pK_a}}\right) \quad (2)$$

Importantly, these values are up to two orders of magnitude higher than that reported for Aβ(1-40) using the same method-

ology, that is, $2.9\times10^{7}\,\text{M}^{-1}$.[41] Therefore, **HWH** and **HK^{C}H** should, in principle, be excellent competitive copper-binding agents to prevent the toxicity of Cu-Aβ assemblies.

It should be noted that the above-mentioned conditional affinity for the Aβ(1-40) fragment differs significantly from the more widely accepted value of about $10^{10}\,\text{M}^{-1}$.[44] This discrepancy seems to be related to the different methodology used, that is, the introduction of strong competitors such as glycine.[44] Further studies, which are beyond the scope of the present work, are certainly required to identify the reason(s) for these discrepancies. Consequently, the conditional affinity constants reported herein, for both the Aβ(1-40) fragment and the tripeptides, cannot be considered as absolute values but rather as relative ones.

The easier and faster data treatment (since the use of a competitor is not needed) and the reproducibility of the methodology employed in the present study make it a practical approach for straightforward comparative studies on the affinity towards copper(II) of chelating compounds.

Being non-emissive, the affinity of **HAH** could not be determined by fluorescence spectroscopy; hence, competitive binding experiments with **HWH** and **HK^{C}H** were carried out to evaluate the relative affinity of **HAH**, by monitoring the intrinsic fluorescence of the emissive tripeptides (viz. **HWH** and **HK^{C}H**). Figure 6c illustrates the intensification of the emissions of **HWH** and **HK^{C}H** upon addition of increasing amounts of **HAH**. It can be seen that most of the emission enhancements occurred in the range 0–1 equiv of added copper(II). The original emissions of **HWH** and **HK^{C}H** were not totally recovered. In fact, only 50% of the original fluorescence was recovered, which may be due (at least in part) to intermolecular interactions between aromatic rings. The quenching efficacy of such supramolecular interactions can be enhanced in the presence of a metal ion, through either conformational or electronic effects. Indeed, blank experiments (without copper) showed emission quenching to a lower extent.

In summary, the copper-binding affinities of the tripeptides described herein follow the trend **HAH** > **HWH** > **HK^{C}H**. The order of magnitude difference in K^{cond} values between **HWH** and **HK^{C}H** may originate from a stability enhancement of the [Cu-**HWH**] complex through secondary interactions involving the aromatic rings.[45]

To evaluate the role played by the His1 residue in the stabilization of the metal–peptide complex, the values of K^{app} and K^{cond} for the tripeptide **GWH** (L-glycidyl-L-tryptophanyl-L-histidine, in which the histidine at position 1 is replaced by a glycine residue), were determined (Figure S13). The decrease in the intrinsic fluorescence of **GWH** upon addition of copper(II) was more gradual than that for its His1 analogue ($K_{sv}=7.7\times10^{4}\,\text{M}^{-1}$), as evidenced in Figure S13, and confirmed by the corresponding K^{app} of $1.48\pm0.23\times10^{6}\,\text{M}^{-1}$ ($r^{2}=0.984$) and K^{cond} of $1.23\pm0.19\times10^{8}\,\text{M}^{-1}$. The order of magnitude lower K^{cond} for the Cu-**GWH** complex, compared with that for Cu-**HWH**, corroborates the significant effect of His1 on the complex stability, even though it is not involved in the coordination sphere of the metal ion. Such stabilizing effects of positively charged residues in copper(II)–peptide complexes exhibiting an albumin-like coordination environment have been mentioned previously by Kozlowski.[6] Furthermore, an improvement of complex stability by aromatic AAs (i.e., Phe, Tyr, or Trp) through direct electronic interactions with the metal ion, π stacking, or general hydrophobic effects has been proposed.[6] At this point, it has to be stressed that, in the present study, the peptide containing a non-aromatic central residue (namely alanine) exhibited better copper(II)-binding properties than its analogous tripeptides containing an aromatic central AA (histidine or coumarin-labeled lysine).

Competitive binding studies between the tripeptides and amyloid proteins [Aβ(1–16) and Aβ(1–42)]: As outlined above, the tripeptides **HWH**, **HK^{C}H**, and **HAH** were selected with the idea of using them as potential binding compounds to compete with amyloid-β fragments for copper. As shown above, the three peptides exhibit Cu^{2+}-binding affinities that are up to two orders of magnitude higher than that displayed by Aβ(1-40). To confirm their higher proficiency to "capture" copper(II) ions, competitive binding experiments were performed using the non-aggregating amyloid fragment Aβ(1-16) ($K^{cond}=1\text{–}2\times10^{7}\,\text{M}^{-1}$),[1] following the intrinsic fluorescence of the tyrosine residue Tyr10 of the protein and the emission of a fluorescent tripeptide. For these studies, **HK^{C}H** was preferred because its emission at 410 nm would not interfere with that of Aβ(1-16) (emission of tyrosine at 305 nm); the excitation wavelength of **HK^{c}H** is far enough from that of Aβ(1-16), in contrast to that for **HWH** ($\lambda_{exc}=275$, 300, and 280 nm for tyrosine, the coumarin group of **HK^{C}H**, and tryptophan, respectively).

In a first experiment, increasing amounts of **HK^{C}H** were added to a solution containing equimolar amounts of copper(II) ions and Aβ(1-16), which had previously been incubated for 2 min (Figure 7a). The Tyr emission of the protein, which was quenched by 40% upon copper binding (Figure 7a), was monitored upon addition of **HK^{C}H**. 90% of the initial fluorescence of Aβ(1-16) was recovered when an equimolar amount of the tripeptide was added to the Cu-Aβ mixture (Figure 7a). This result indicated that the metal ion was displaced from the protein by the tripeptide. At higher peptide concentrations (> 1 equiv **HK^{C}H**), the emission of the protein showed a linear decrease. This effect was also observed in a blank experiment employing only Aβ(1-16) and **HK^{C}H** (i.e., without copper); hence, an energy-transfer process between the emission of Tyr at 305 nm and the absorption of the coumarin fluorophore at 300 nm may justify this (FRET-type) phenomenon. This assumption was reinforced by a similar titration carried out by gradually adding non-emissive **HAH** peptide to a solution of the Cu-Aβ(1-16) complex (Figure S14), in which case no energy transfer could take place because of the absence of an acceptor. Indeed, 100% of the amyloid protein emission was recovered after the addition of an equimolar amount of peptide, and the emission remained relatively constant on adding excess **HAH** (Figure S14).

Subsequently, a reverse experiment was performed in which increasing amounts of Aβ(1-16) were added to a solution of Cu-**HK^{C}H**. As anticipated, the emission of the coumarin moiety increased linearly and in a less pronounced fashion than in the

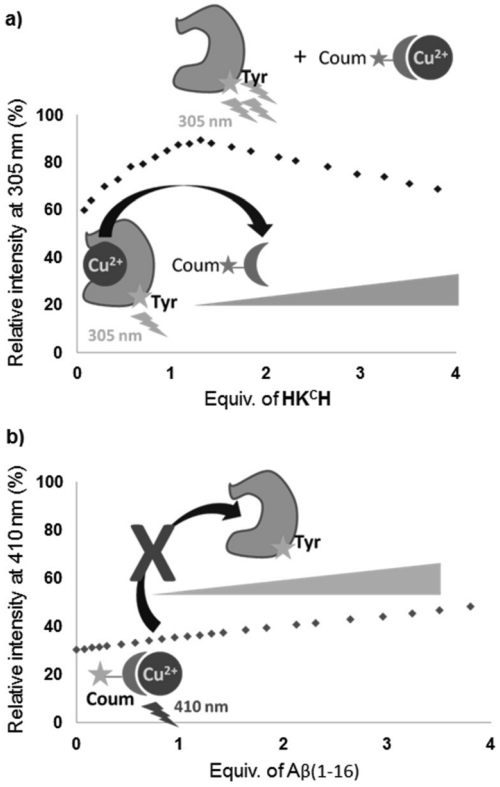

Figure 7. Competitive fluorescence titration studies between **HK^{C}H** and the Aβ(1-16) fragment: a) addition of increasing amounts of **HK^{C}H** to Cu-Aβ(1-16) ([Cu-Aβ(1-16)] = 10 μM) in HEPES (10 mM, pH 7.4); b) addition of increasing amounts of Aβ(1-16) to Cu-**HK^{C}H** ([Cu-**HK^{C}H**] = 10 μM) in HEPES (10 mM, pH 7.4).

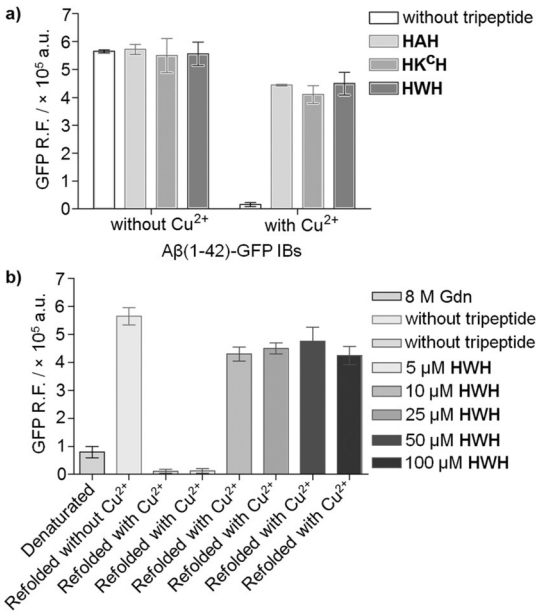

Figure 8. Competitive copper(II)-binding studies between the tripeptides and Aβ(1-42). a) Recovery of GFP fluorescence of Aβ(1-42)–GFP fusion constructs through the formation of Cu^{II}-**HWH**, Cu^{II}-**HAH**, or Cu^{II}-**HK^{C}H** 1:1 complexes; [tripeptide] = [Cu^{II}] = 10 μM. b) Effect of the addition of increasing concentrations of **HWH** ([**HWH**] = 5–100 μM) on the recovery of GFP fluorescence of Aβ(1-42)–GFP fusion constructs, confirming the preferential formation of a 1:1 Cu^{II}-tripeptide species; [Cu^{II}] = 10 μM.

previous experiments (Figure 7b). Furthermore, no slope change was observed in the plot (Figure 7b), and the corresponding blank measurements presented a similar profile. These features corroborated the high stability/inertness of the Cu-**HK^{C}H** complex, even in the presence of up to four equivalents of the protein. As proposed earlier (see above), the data obtained from the blank experiment can be explained by an energy-transfer process from the Tyr10 residue to the coumarin group. It may be noted that, in the respective cases, the value of the slope is equivalent but with opposite sign (about 10% per added equivalent of the titrant). Finally, it may be noted that, since **HK^{C}H** showed the lowest binding affinity among the three peptides investigated, it can be surmised that **HAH** (Figure S14) and **HWH** will be even better Aβ(1-16) competitors.

Next, aggregation studies were carried out through competitive binding between the tripeptides and GFP-conjugated Aβ(1-42) (Aβ42-GFP) inclusion bodies.[46] In the absence of copper(II) ions, an increase in GFP fluorescence (λ_{exc} = 488 nm; λ_{em} = 512 nm) of the Aβ42-GFP fusion construct was observed over time as the fusion protein was refolded (Figure 8a), indicative of a normal refolding of the GFP. The addition of **HWH**, **HK^{C}H**, or **HAH** did not affect the aggregation of Aβ42-GFP (Figure 8a), suggesting that the tripeptides do not directly interfere with the amyloid aggregation process. Remarkably, when a solution of copper(II) ions (10 μM) was added to a denatured solution of Aβ42-GFP, a drastic reduction of GFP fluorescence occurred with the refolding process (Figure 8a), attributable to the rapid aggregation of a copper(II)/Aβ42-GFP species that prevents correct refolding of the GFP. Subsequently, experiments were performed in which 10 μM solutions of the different tripeptides were added to a copper(II)/Aβ42-GFP solution (copper-to-tripeptide ratio of 1:1). In all cases, about 80% of the GFP fluorescence was observed (indicating the occurrence of GFP refolding), thus confirming a preferential binding of the copper(II) ions to the tripeptides as opposed to Aβ(1-42) (Figure 8a).

To evaluate the inhibitory effect of increasing amounts of peptide on Aβ(1-42) aggregation, **HWH** in the concentration range 5–100 μM was added to a copper(II)/Aβ42-GFP solution with [Cu^{2+}] = 10 μM. The corresponding results are depicted in Figure 8b; it can clearly be seen that an equimolar amount of tripeptide (i.e., a minimum concentration of 10 μM) was required to recover about 80% of the fluorescence of GFP (occurring through appropriate protein folding). An [**HWH**] of 5 μM did not allow recovery of the normal aggregation of the protein (Figure 8b). It may also be noted that complete recovery of the GFP fluorescence could not be achieved, even in the presence of an excess of tripeptide (Figure 8b). This may be explained by some GFP fluorescence quenching induced by the presence of copper(II) ions in the mixture.

Aggregation kinetic studies with Aβ(1–40): Next, the time-dependent aggregation of Aβ(1-40) without and with copper(II) ions was monitored by using thioflavin T (ThT) fluorescence, which increases substantially upon binding to aggregated fibrillar structures forming β sheets.[47] Without copper, only

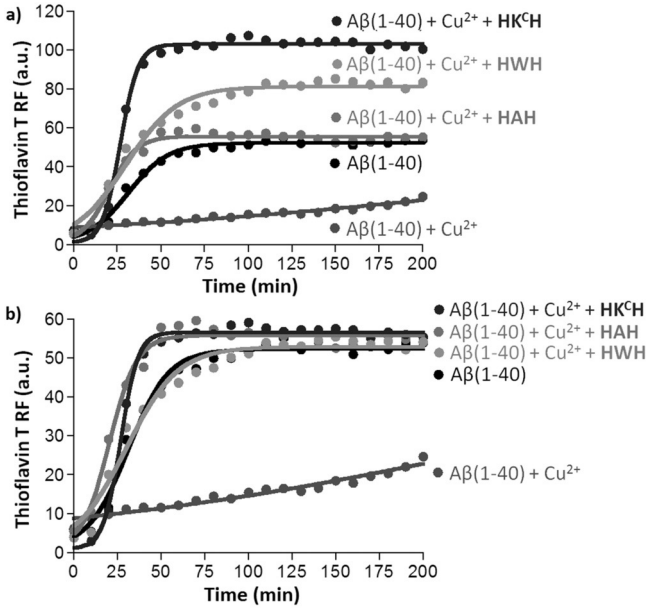

Figure 9. Time course of Aβ(1-40) aggregation: a) ThT fluorescence data ($\lambda_{exc} = 445$ nm; $\lambda_{em} = 480$ nm) obtained for free Aβ(1-40), Aβ(1-40) in the presence of Cu^{2+} ions, and of Aβ(1-40) + Cu^{2+} in the presence of the different tripeptides; b) corrected fluorescence data taking into account the fluorescence enhancement occurring upon interaction of the tripeptides with ThT-Aβ formed in the presence of Cu^{2+} ions (see text for details and Figure 10).

a weak ThT signal was observed with a freshly dissolved protein (see Figure 9). Upon incubation, a short lag phase (or nucleation phase) was observed, immediately followed by an elongation phase (or growth phase) until the saturation phase (after about 75 min; see Figure 9), whereupon large fibrils were generated.[48] The resulting sigmoidal curve was typical for the aggregation (fibrillation) process of amyloid-β (and more generally of amyloidogenic proteins).[49] In the presence of copper(II) (one equivalent), completely different behavior was observed (Figure 9). As reported in the literature, copper(II) ions prevent the formation of β-sheet-rich assemblies (which are ThT-positive),[50] most likely stabilizing metal-oligomeric species.[51] It may also be noted that, after 3 h of incubation, the ThT fluorescence started to rise, and after 8 h reached an intensity comparable to that achieved without copper (see Figure S15). Thus, copper clearly retards the formation of amyloid fibrils.

Subsequently, the effects of the tripeptides on the aggregation process were investigated by monitoring the ThT fluorescence of a solution containing one equivalent of Aβ(1-40), one equivalent of copper(II) ions, and two equivalents of tripeptide His-Xaa-His (Xaa = tryptophan, N^{ε}-coumarin-labeled lysine, or alanine), added concurrently. Interestingly, with each of the three tripeptides, sigmoidal kinetic curves were obtained (Figure 9a, for Xaa = **W**, **K^{C}**, and **A**), similar to what was observed without copper (Figure 9). Accordingly, the tripeptides are all capable of capturing copper(II) ions, which therefore do not affect the aggregation/fibrillation of Aβ(1-40). Surprisingly, higher fluorescence intensities (compared with that of free Aβ(1-40)) were obtained with **HK^{C}H** and **HWH** (Figure 9a). As this increased ThT fluorescence may be explained by the involvement of the fluorescent tryptophan (**HWH**) or coumarin (**HK^{C}H**) group (for instance, through a Förster resonance energy transfer (FRET) process), the ThT fluorescence of preformed Aβ(1-40) fibrils (without copper) upon addition of each tripeptide was examined (Figure 10a). The corresponding results clearly showed that all three tripeptides had no effect on the fluorescence of the ThT-Aβ assemblies (Figure 10a), suggesting no interaction between them and ThT. Therefore, a FRET-type process between the peptides and ThT may be discarded.

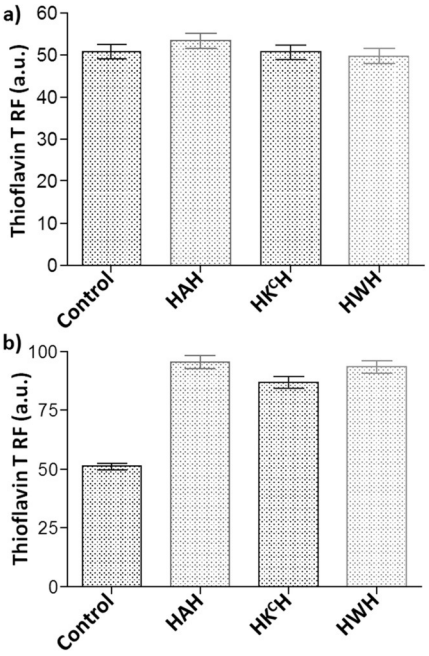

Figure 10. Effects of the tripeptides on the fluorescence of ThT-containing Aβ(1-40) fibers: a) Aβ(1-40) fibers pre-formed without copper in water (control) or mixed with **HAH**, **HK^{C}H**, or **HWH**; b) Aβ(1-40) fibers pre-formed in the presence of Cu^{2+} ions in water (control) or mixed with **HAH**, **HK^{C}H**, or **HWH** (see Experimental Section for details).

In contrast, when ThT-Aβ fibrils were obtained after incubation for 24 h in the presence of copper(II) ions (see Figure S15), a significant augmentation of ThT fluorescence (with respect to that of ThT-Aβ fibrils obtained without copper(II)) was observed for **HK^{C}H**, **HWH**, and **HAH** (Figure 10b). Correction for this additional ThT fluorescence in the kinetic curves for **HWH** and **HK^{C}H** (Figure 9a) generated sigmoidal curves (Figure 9), similar to that obtained for Aβ(1-40) (Figure 9). The fact that no ThT fluorescence increase was observed for **HAH** (Figure 9) confirmed the higher affinity of this tripeptide for copper(II) (see above). In fact, it appears that upon concurrently mixing Aβ(1-40), ThT, **HAH**, and the copper salt, the copper(II) ions are immediately trapped by the tripeptide, thus impeding the ThT fluorescence enhancement that was observed upon addition of **HAH** to pre-formed ThT-Aβ fibrils in the presence of this metal (Figure 10b). In other words, since copper is instantly bound by **HAH** (due to its high affinity), the cations have no time to form the species with enhanced ThT emission (Fig-

ure 10b), and a "normal" fibrillation pathway (i.e., that observed for ThT-Aβ assemblies obtained in the absence of copper; Figure 9) is followed.

As a matter of fact, the unexpected augmentation of ThT fluorescence illustrated in Figure 10b is very informative; first, these data indicate that the tripeptides are able to bind and thus remove copper(II) ions from amyloid β-sheet structures, which is a very interesting feature in the context of potential applications of such small peptides in AD. Second, the fluorescence increase (which reaches a level significantly higher than that achieved without copper) after copper removal (by the tripeptides) suggests that the Aβ fibers generated in the presence of the metal contain pre-organized structures that most likely produce a higher-level association of the protein when the copper(II) ions are removed, leading to enhanced ThT emission. In-depth studies (which are beyond the scope of the present work) are clearly required to investigate this remarkable process.

Inhibition of ROS production/release: Besides their involvement in Aβ aggregation, redox-active copper(II) ions can also induce oxidative stress (leading to cell death). In the presence of biological reductants (e.g., ascorbate), Cu^{II}-Aβ is more toxic than Aβ alone. The toxic effects of copper(II) are specific to its interaction with Aβ(1-40) and Aβ(1-42),[52] which gives rise to the generation of ROS, thereby inducing oxidative stress. Therefore, the administration of a well-designed copper(II) chelator may have a dual function, namely the removal of Aβ-bound copper(II) ions and the blocking/lessening of oxidative stress.

The effects of the tripeptides on the copper-catalyzed production of ROS were first evaluated at physiological concentrations of ascorbate (i.e., 100 μM) by monitoring its consumption through its absorbance at 265 nm over a period of 30 min following its addition (Figure 11a). Whilst a significant decrease in ascorbate was observed when free copper(II) ions were used, the sole addition of 1.1 equiv (with respect to copper) of any of the three peptides and Aβ(1-40) led to a drastic diminution of ROS production (Figure 11a). Both **HK^{C}H** and **HWH** served as very efficient ROS inhibitors, since 97% and 95% inhibitions, respectively, were achieved after 30 min (see the Experimental Section for details), whereas high amounts of ROS were produced in the case of free copper(II) (see the respective plots in Figure 11a). **HAH** proved to be a slightly less efficient inhibitor of ROS formation, with 85% inhibition. These data are in sharp contrast to the intrinsic ROS generation from the Cu/Aβ(1-40) complex and the redox cycling of "free" copper(II) ions, which consumed 38% and 73%, respectively, of the initial amount of ascorbate.

Next, the potential formation of hydroxyl radicals (HO•), which represent the ultimate, very harmful ROS produced through Cu^{II}/Cu^{I} redox cycling (see Figure 11a), was investigated. To this end, the generation of HO• in the presence of the natural reducing agent ascorbate under aerobic conditions was monitored indirectly through the formation of 7-hydroxy-coumarin-3-carboxylate (7-OHCCA) from coumarin-3-carboxylate (3-CCA). The characteristic emission of 7-OHCCA at 500 nm was used to monitor its formation over a period of 30 min following the addition of ascorbate. The 7-OHCCA emission of a micromolar solution of copper(II) ions containing 1.1 equiv of tripeptide was strongly inhibited compared to that in the case of a solution of free copper(II), that is, without added peptide or amyloid protein (Figure 11b). The three peptides exhibited comparable efficiencies, with degrees of inhibition ranging from 67% to 76% after 30 min. In comparison, Aβ(1-40) led only to 12% inhibition after the same duration. Moreover, it should be noted that the inhibition rates of hydroxyl radical formation are lower than those for total ROS formation (cf. the ascorbate consumption experiments above). This apparent discrepancy may be due to the fact that a three-fold higher

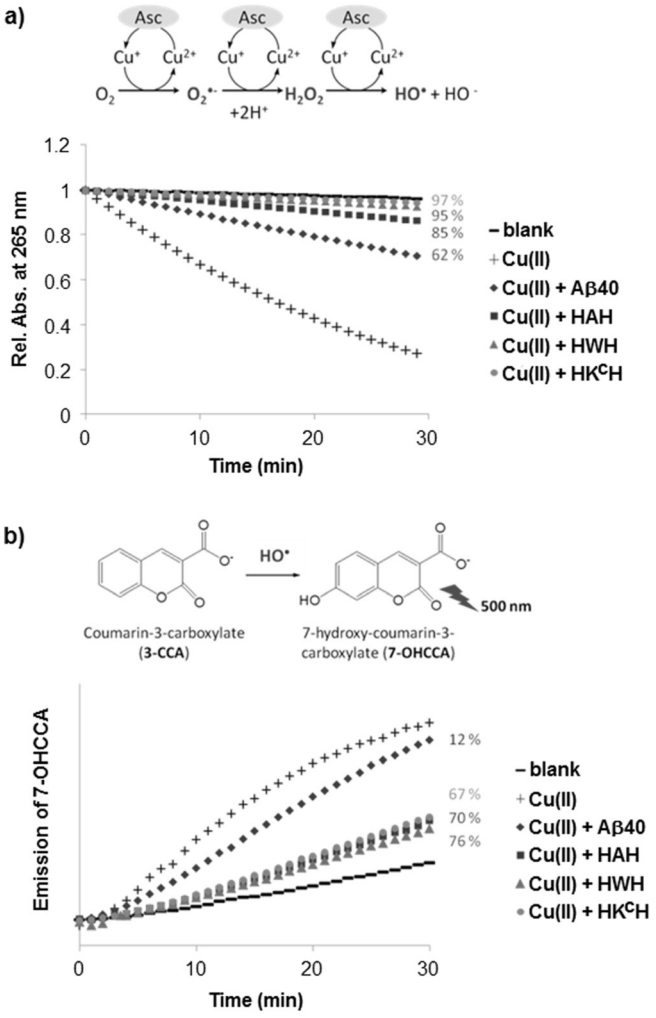

Figure 11. a) ROS formation mediated by the Cu^{II}-peptide complexes and by $CuCl_2$, determined by the consumption of ascorbate through its maximum absorbance at 265 nm; [$CuCl_2$] = 1 μM, [peptide] = 1.1 μM, [ascorbate] = 100 μM, phosphate buffer 100 mM, pH 7.4. The blank experiment was performed under the same conditions but in the absence of copper(II) and peptide/protein. b) Effects of the Cu^{II}-peptide complexes on the Cu^{II}-mediated production of HO•, measured by the characteristic fluorescence of 7-hydroxy-coumarin-carboxylate (7-OHCCA) formed by reaction of HO• with 3-coumarin-carboxylate (3-CCA); λ_{ex} = 385 nm, λ_{em} = 500 nm, [$CuCl_2$] = 1 μM, [peptide] = 1.1 μM, [ascorbate] = 300 μM, [3-CCA] = 1 mM. Phosphate buffer: 100 mM, pH 7.4. The blank experiment was carried out under the same conditions but in the absence of copper(II) and peptide/protein. The inhibition percentages are indicated next to the respective curves.

amount of ascorbate (i.e., [ascorbate] = 300 μM) was used in these experiments (cf. [ascorbate] = 100 μM for the previous studies; see above). It should also be stressed that this excess of ascorbate appeared to strongly affect the reaction mixture containing Aβ(1-40). The obtained results also revealed that the (prospective) peptide-mediated scavenging of hydroxyl radicals is negligible compared to the inhibition of total ROS production.

In summary, **HK^{C}H**, **HWH**, and **HAH** are capable of significantly hampering the total production of ROS, including HO$^\bullet$, which is one of the most destructive radicals found in biology.[53] Interestingly, the inhibition of these very harmful copper-catalyzed oxidative processes is notable when the copper(II) ions are captured by the tripeptides (as compared to the amyloid protein).

Conclusion

There is evidence that amyloid-β aggregation and the associated neurotoxicity are related to copper dyshomeostasis as well as that of other metals such as zinc and iron.[2,54] However, the possible interrelation between the different levels of these metal ions in the brain has yet to be fully elucidated. Likewise, the actual sequential correlation of metal misbalance with characteristic features of Alzheimer's disease, such as amyloid aggregation or tau hyperphosphorylation, is unclear. Nevertheless, targeting one of these metal ions (e.g., to restore intracellular metallostasis), for instance copper, may have a positive impact on the levels of the others and on the progression of the disease. Indeed, copper chelators, for example clioquinol, have already been used in vivo with some promising effects.[55]

In the present study, small and simple oligopeptides have been designed to chelate copper(II) ions. Investigation of their metal-binding properties has revealed that these tripeptides of the sequence H-His-Xaa-His-OH exhibit an albumin-like binding mode, which is typical of His3 peptides.[56] However, these highly stable CuN_4 species are not conserved at elevated peptide-to-copper molar ratios, converting to a CuN_3O_2 motif involving the coordination of at least two peptidic molecules. At equimolar copper-to-peptide ratios, the His1 residue, despite not being directly bound to Cu^{II}, confers an additional stability to the ATCUN-type complexes formed. The central AA also plays a role in the binding affinity to copper, probably through secondary interactions involving steric aspects and the aromatic rings. The conditional affinity constants of the three peptides have been determined by intrinsic fluorescence measurements, and are two orders of magnitude higher than that previously reported for Aβ(1-40). Competitive binding studies based on fluorescence measurements using either Aβ(1-16) or bacterial inclusion bodies of Aβ42-GFP have confirmed their efficient ability to displace Aβ-bound Cu^{II} ions in an irreversible fashion. ThT emission studies have suggested that copper-induced oligomer aggregation of Aβ(1-42) is indeed inhibited in the presence of the peptides, and on adding the peptides to Cu-induced fibrils a modulation of such fibrillation occurred. The striking enhancement of ThT fluorescence upon interaction of the tripeptides with ThT-Aβ fibrils preformed in the presence of copper is being investigated.

Finally, the tripeptides are capable of markedly hindering the redox activity of copper(II) ions and the associated ROS production, especially in comparison with Aβ(1-40). The similarity in the inhibition rates induced by **HAH**, **HWH**, and **HK^{C}H** points to the binding mode as the main factor regulating the copper(II) activity. In agreement with previous reports,[16] the present work has confirmed that the ATCUN motif is an extremely effective redox-silencing unit, which may therefore be used to diminish the oxidative stress caused by mislocalized copper in the brain.

These peptidic sequences may represent potential synthons for the design of copper ionophores, which may redistribute this metal ion in AD-affected brains.

Experimental Section

Materials: The tripeptides **HWH**, **HAH**, and **GWH** were custom-made by GeneCust (Luxembourg), and were received as hydrochloride salts with purity ≥95%. These peptides were used without further purification. $CuCl_2{\cdot}2H_2O$ was used as a source of copper(II) ions in all of the studies.

The tripeptide H-His-Lys(coum)-His-OH (**HK^{C}H**) was synthesized by a solid-phase synthetic method with Fmoc-amino acids and a 2-chlorotrityl chloride (2-CTC) resin. The non-natural fluorescent amino acid N$^\alpha$-Fmoc-N$^\varepsilon$-(coumarin-3-ylcarbonyl)-L-lysine was synthesized following the procedure described by Katritzky et al.[57] Thus, **HK^{C}H** was built-up on a solid support in a linear fashion; the first AA was coupled to the resin using *N*,*N*-diisopropylethylamine (DIPEA). After a reaction time of 100 min, the subsequent AAs were coupled with a threefold excess of *N*,*N*′-diisopropylcarbodiimide and ethyl 2-cyano-2-(hydroxyimino)acetate (DIC/Oxyma) for 1 h using a threefold excess of the AA in DMF/CH_2Cl_2 (1:1), with alternate washings with DMF and CH_2Cl_2. Next, the Fmoc groups were removed by treatment (5×10 min) with piperidine/DMF (20:80). The progress of each coupling reaction was monitored by the ninhydrin test (Kaiser test[58]). The final tripeptide was cleaved from the resin by treatment with TFA/TIPS/CH_2Cl_2 (40:5:55) for 45 min, washed with TFA/CH_2Cl_2 (1:1), and collected by precipitation with Et_2O. The purity of the peptide was checked by HPLC; in the case of purity below 95%, further purification by means of preparative reversed-phase HPLC was carried out.

In all studies carried out with these peptides, the concentrations of the prepared stock solutions were checked spectrophotometrically, using the molar absorptivity values ε(Trp, 280 nm) = 5690 $M^{-1}cm^{-1}$[59] and ε(Lys(coumarin), 300 nm) = 12271 $M^{-1}cm^{-1}$.

UV/Vis absorption and circular dichroism spectroscopies: UV/Vis absorption spectra were recorded on a Varian Cary 100 Scan spectrophotometer at room temperature employing a 1 cm pathlength cuvette. A JASCO J-815 circular dichroism spectropolarimeter was used to acquire CD spectra at room temperature at different Cu^{II}-to-peptide ratios, with a scanning speed of 200 nm min^{-1} and 1 cm pathlength cuvettes. 1 mM peptide solutions were prepared for the UV/Vis absorption studies. For the CD experiments, 0.125 mM solutions were used. In all cases, the solutions were prepared in HEPES buffer (100 mM, pH 7.4).

Consumption of ascorbate: Absorbance measurements at 265 nm (which corresponds to the maximum absorption peak of ascorbate) were carried out under aerobic conditions at room temperature in

100 mM phosphate buffer (pH 7.4). The buffer solution had been pre-treated with Chelex 100 resin (Bio-Rad) to remove any metal traces. The absorbance was registered over a 30 min time span. The inhibition rates were calculated according to Equation (3):

$$\%\text{inhibition} = (1 - \frac{\text{Abs} - \text{Abs}_{\text{blank}}}{\text{Abs}_{\text{freeCu}} - \text{Abs}_{\text{blank}}})\text{x}100 \quad (3)$$

Electrospray ionization mass spectrometry: ESI mass spectra were recorded on an LC/MSD-TOF spectrometer (Agilent Technologies) equipped with an electrospray ionization (ESI) source at the Serveis Cientificotècnics of the Universitat de Barcelona. The spectra were acquired in positive-ion mode at either 175 or 215 V. The solutions were prepared in Milli-Q water, with $[CuCl_2] = 0.5$ mM, [peptide] = 0.25 mM, and pH 7.4 (adjusted with NaOH).

Fluorescence spectroscopy: Fluorescence measurements were carried out using a HORIBA Jobin–Yvon iHR320 spectrofluorimeter at room temperature. The photomultiplier detector voltage was set at 950 V and the instrument excitation and emission slits were both set at 5 nm. In all cases, the pH was fixed at 7.4 with 100 mM HEPES buffer, except in the competition studies, for which 10 mM HEPES was employed instead.

Calculation of the conditional binding constants: The apparent affinity constants of the Cu^{II} complexes with **HWH** and **HK^{c}H** were calculated by fitting the fluorescence titration data to Equation (1) (see above).[41,42] Since HEPES, the buffer used for the measurements, can form a 1:1 complex with copper(II) and can thus act as a weak competitor, its influence on the binding equilibrium had to be taken into account. Therefore, the affinity constants at zero buffer concentration, that is, the conditional binding constants (K^{cond}), were determined. For very large quantities of HEPES with respect to the other components in the solution, Equation (2) (see above) can be applied.[43]

Generation of hydroxyl radicals; formation of 7-hydroxy-coumarin-carboxylic acid (7-OHCCA): Single-point fluorescence measurements were performed at room temperature in phosphate buffer (100 mM, pH 7.4). The buffer solution had been pre-treated with Chelex 100 resin (Bio-Rad) to remove any metal traces. The samples were excited at 385 nm and the emission at 500 nm was registered over a period of 30 min, under aerobic conditions. A 5 mM stock solution of 3-coumarin-carboxylic-acid (3-CCA) was prepared in phosphate buffer as described previously.[53] An ascorbate solution was freshly prepared in phosphate buffer immediately prior to each measurement. The final concentrations used for the assays were 1 μM $CuCl_2$, 1.1 μM peptide, 300 μM ascorbic acid, and 1 mM 3-CCA. The inhibition rates were calculated according to Equation (4):

$$\%\text{inhibition} = (I - \frac{I - I_{\text{blank}}}{I_{\text{freeCu}} - I_{\text{blank}}})\text{x}100 \quad (4)$$

NMR studies: 1D and 2D NMR experiments were performed on a Bruker Avance III 400 MHz spectrometer, equipped with a 5 mm cryoprobe (Prodigy) broadband (CPPBBO BB-^{1}H/^{19}F/D) with gradients in *Z*, at the Centres Científics i Tecnològics of the Universitat de Barcelona (CCiTUB). Solvent suppression for the 1D experiments was achieved using a PRESAT pulse sequence. The NMR data were analyzed using MestReNova 9.1.0. Solutions of 10 mM peptide in D_2O were adjusted to pH 7.4, and measured with an insert containing a 5 mg mL^{-1} solution of [D_4]-3-(trimethylsilyl)propanoic acid (TSP) as an internal reference. In the presence of 0.01 equiv of Cu^{II} ions, the intensity of the peptide NMR signals decreased by about 60%.

The ^{1}H and ^{13}C signals of the peptides were assigned on the basis of ^{1}H-^{1}H COSY, ^{1}H-^{13}C HSQC, and ^{1}H-^{13}C HMBC experiments. It should be noted that, even though the measurements were made in D_2O, it was decided to use the notation pH.

EPR studies: X-band EPR spectra of frozen solutions were recorded at 77 K on a Bruker ESP300E spectrometer. WINEPR 2.11 software (Bruker) was used to process and simulate the spectra. Aqueous $CuCl_2$/peptide mixtures in ratios of 1:1.1 (5 mM Cu^{2+}) and 1:100 (2 mM Cu^{2+}) were used in 100 mM HEPES buffer (pH 7.4).

Competitive binding studies using GFP-Aβ(1–42) fusion constructs

Production and purification of bacterial inclusion bodies (IBs): Escherichia coli competent cells BL21 (DE3) were transformed with the pET28a vector from Novagen (Merck KGaA, Darmstadt, Germany) carrying the DNA sequence of the Aβ42-GFP fusion protein. The Aβ protein produced by the bacteria contains an additional methionine residue at its N terminus for the addition of the initiation codon ATG in front of the gene; hence, the sequence of the resulting [Met + Aβ(1–42)] peptide is

Met - Asp - Ala - Glu - Phe - Arg - His - Asp - Ser - Gly - Tyr - Glu - Val - His - His - Gln - Lys - Leu - Val - Phe - Phe - Ala - Glu - Asp - Val - Gly - Ser - Asn - Lys - Gly - Ala - Ile - Ile - Gly - Leu - Met - Val - Gly - Gly - Val - Val - Ile - Ala. Over-expression of the Aβ42-GFP fusion constructs was carried out as described previously.[60] Briefly, bacterial cultures (10 mL) were grown overnight at 37 °C and 250 rpm in Luria broth (LB) medium containing 50 μg mL^{-1} kanamycin. For the protein over-expression, these cultures (10 mL) were inoculated into LB (1 L) containing 50 μg mL^{-1} of kanamycin. At an absorbance at 600 nm of 0.8, 1 mM isopropyl-β-D-1-thiogalactopyranoside (IPTG) was added to induce recombinant protein expression. After 4 h, the bacterial cells were harvested by centrifugation, and the obtained pellets were re-suspended in lysis buffer containing 100 mM NaCl, 1 mM EDTA, and 50 mM Tris at pH 8 to purify the intracellular inclusion bodies (IBs), as described previously.[19] The IBs were purified by a differential centrifugation/detergent washing procedure.[61,62] In brief, the protease inhibitor PMSF and lysozyme were added so as to give final concentrations of 15 mM and 300 μg mL^{-1}, respectively. The samples were then incubated at 37 °C for 30 min. Subsequently, 1% NP-40 was added and the mixture was incubated at 4 °C for 50 min under gentle agitation. In order to remove nucleic acids, the cells were treated with 15 μg mL^{-1} DNase and RNase at 37 °C for 30 min. Finally, the IBs were collected by centrifugation at 12,000 *g* for 10 min and washed with lysis buffer containing 0.5% Triton X-100. In a last step, the samples were washed three times with PBS.[62]

In vitro refolding assay of Aβ42-GFP inclusion bodies: Purified IBs were concentrated by centrifugation to an absorptivity of 100 at 360 nm. Then, 10 μL of IBs was centrifuged and the pellets were re-suspended in 10 μL of 8 M guanidine (Gdn·HCl) and incubated at room temperature for 4 h under mild agitation and sonication. For the refolding process, 10 μL of denatured IBs was dissolved in 990 μL of refolding buffer. These buffers were prepared from PBS that had been pre-treated with Chelex 100 from Sigma–Aldrich (St. Louis, MO, USA). When required, 10 μL of refolding buffer was replaced by 10 μL of 1 mM $CuCl_2$ so as to give a final metal concentration of 10 μM. In the same manner, 10 μL aliquots of **HWH**, **HK^{c}H**, or **HAH** from 1 mM stock solutions were added to the sample. The samples were then incubated at room temperature for 16 h (overnight) under mild agitation. The GFP fluorescence of the solutions containing refolded IBs was measured with an Aminco Bowman Series 2 luminescence spectrophotometer (Aminco-Bowman AB2, SLM Aminco, Rochester, NY, USA), using excitation and emission wavelengths of 488 nm and 512 nm, respec-

tively, and slit widths of 4 nm. All measurements were performed in triplicate.

***In vitro* Aβ(1–40) aggregation kinetics**

Preparation of aggregate-free amyloid-β peptide: Aβ(1–40) peptide was obtained from Bachem (Bubendorf, Switzerland). Aβ(1–40) (1 mg) was solubilized in 1,1,1,3,3,3-hexafluoro-2-propanol (HFIP; 500 μL) under vigorous stirring at room temperature for 1 h. The resulting solution was sonicated for 30 min and subsequently stirred at room temperature for a further 1 h. The solution was then maintained at 4 °C for 30 min to avoid solvent evaporation during aliquot collection. To eliminate possible insoluble materials, the samples were passed through 0.22 μm filters. Lastly, aliquots of soluble Aβ(1–40) were collected and HFIP was evaporated under a gentle stream of nitrogen. The samples were stored at −20 °C.

Aggregation studies: The samples were re-suspended in dimethyl sulfoxide (DMSO; 50 μL), and the monomers were solubilized through sonication for 10 min. 100 μL of 250 μM ThT, 100 μL of 100 mM Tris-HCl buffer (pH 7.4), and the appropriate amount of MilliQ water were then added to obtain final solutions of 20 μM Aβ(1–40) and 25 μM ThT in 10 mM Tris-HCl containing 5% (v/v) DMSO. When required, pure MilliQ water was replaced by the same volume of a solution of $CuCl_2$ to obtain a final $[Cu^{2+}]$ of 20 μM. Similarly, stock solutions of **HAH**, **HK^{C}H**, and **HWH** were added to obtain final concentrations of 40 μM to investigate the effects of the tripeptides on the aggregation process. For the kinetic assays, the samples were placed in a thermomixer (Eppendorf, Germany) at 37 °C and stirred at 1400 rpm; the course of the aggregation was then tracked by detecting ThT fluorescence (λ_{exc} = 445 nm; λ_{em} = 480 nm) using an Aminco Bowman Series 2 luminescence spectrophotometer (Aminco-Bowman AB2, SLM Aminco, Rochester, NY, USA).

To investigate the effects of the different tripeptides on ThT fluorescence of fibrillar Aβ assemblies (containing ThT), Aβ(1–40) fibers ([Aβ] = 20 μM) were pre-formed in the absence and presence of copper ($[Cu^{2+}]$ = 20 μM). These fibers were then mixed with pure water or with 40 μM solutions of **HAH**, **HK^{C}H**, or **HWH** for 90 min. It should be noted that pre-formed fibers were obtained in the absence or presence of copper ($[Cu^{2+}]$ = 20 μM) after incubation for 24 h at 37 °C and under stirring at 1400 rpm.

Acknowledgements

The Ministerio de Economía y Competitividad of Spain (Projects CTQ2014-55293-P and CTQ2015-70371-REDT) and COST Action (CM1105) are kindly acknowledged. PG acknowledges the Institució Catalana de Recerca i Estudis Avançats (ICREA). PG, ABC, AE, and RS thank the Institute of Nanoscience and Nanotechnology (IN_2UB). RS is the beneficiary of a contract under the Ramón y Cajal programme (RYC-2011-07987), while AE is the beneficiary of a contract under the Juan de la Cierva programme (JCI-2012-12193), both financed by the Ministerio de Economía y Competitividad of Spain (MINECO).

Keywords: aggregation · amyloid oligomers · copper · metal homeostasis · neurodegenerative disease · oxidative stress

[1] P. Gamez, A. B. Caballero, *AIP Adv.* **2015**, *5*, 092503.
[2] M. A. Lovell, J. D. Robertson, W. J. Teesdale, J. L. Campbell, W. R. Markesbery, *J. Neurol. Sci.* **1998**, *158*, 47–52.
[3] A. I. Bush, *Trends Neurosci.* **2003**, *26*, 207–214.
[4] M. E. Larson, S. E. Lesne, *J. Neurochem.* **2012**, *120*, 125–139.
[5] C. Hureau, P. Faller, *Biochimie* **2009**, *91*, 1212–1217.
[6] H. Kozlowski, W. Bal, M. Dyba, T. Kowalik-Jankowska, *Coord. Chem. Rev.* **1999**, *184*, 319–346.
[7] S. T. Prigge, A. S. Kolhekar, B. A. Eipper, R. E. Mains, L. M. Amzel, *Science* **1997**, *278*, 1300–1305.
[8] S. T. Prigge, R. E. Mains, B. A. Eipper, L. M. Amzel, *Cell. Mol. Life Sci.* **2000**, *57*, 1236–1259.
[9] J. E. Gleason, A. Galaleldeen, R. L. Peterson, A. B. Taylor, S. P. Holloway, J. Waninger-Saroni, B. P. Cormack, D. E. Cabelli, P. J. Hart, V. C. Culotta, *Proc. Natl. Acad. Sci. USA* **2014**, *111*, 5866–5871.
[10] R. L. Lieberman, A. C. Rosenzweig, *Nature* **2005**, *434*, 177–182.
[11] L. Hesse, D. Beher, C. L. Masters, G. Multhaup, *FEBS Lett.* **1994**, *349*, 109–116.
[12] A. Messerschmidt, R. Huber, *Eur. J. Biochem.* **1990**, *187*, 341–352.
[13] G. Y. Park, J. Y. Lee, R. A. Himes, G. S. Thomas, N. J. Blackburn, K. D. Karlin, *J. Am. Chem. Soc.* **2014**, *136*, 12532–12535.
[14] L. Pickart, M. M. Thaler, *Nature New Biol.* **1973**, *243*, 85–87.
[15] A. Trapaidze, C. Hureau, W. Bal, M. Winterhalter, P. Faller, *J. Biol. Inorg. Chem.* **2012**, *17*, 37–47.
[16] C. Hureau, H. Eury, R. Guillot, C. Bijani, S. Sayen, P. L. Solari, E. Guillon, P. Faller, P. Dorlet, *Chem. Eur. J.* **2011**, *17*, 10151–10160.
[17] M. Mylonas, J. C. Plakatouras, N. Hadjiliadis, A. Krezel, W. Bal, *Inorg. Chim. Acta* **2002**, *339*, 60–70.
[18] M. Mital, N. E. Wezynfeld, T. Fraczyk, M. Z. Wiloch, U. E. Wawrzyniak, A. Bonna, C. Tumpach, K. J. Barnham, C. L. Haigh, W. Bal, S. C. Drew, *Angew. Chem. Int. Ed.* **2015**, *54*, 10460–10464.
[19] M. Dasari, A. Espargaro, R. Sabate, J. M. L. del Amo, U. Fink, G. Grelle, J. Bieschke, S. Ventura, B. Reif, *ChemBioChem* **2011**, *12*, 407–423.
[20] N. S. de Groot, F. X. Aviles, J. Vendrell, S. Ventura, *FEBS J.* **2006**, *273*, 658–668.
[21] S. S. S. Wang, Y. T. Chen, S. W. Chou, *Biochim. Biophys. Acta-Mol. Basis Dis.* **2005**, *1741*, 307–313.
[22] P. M. H. Kroneck, V. Vortisch, P. Hemmerich, *Eur. J. Biochem.* **1980**, *109*, 603–612.
[23] H. Sigel, R. B. Martin, *Chem. Rev.* **1982**, *82*, 385–426.
[24] E. Prenesti, P. G. Daniele, S. Berto, S. Toso, *Polyhedron* **2006**, *25*, 2815–2823.
[25] A. Myari, G. Malandrinos, Y. Deligiannakis, J. C. Plakatouras, N. Hadjiliadis, Z. Nagy, I. Sovago, *J. Inorg. Biochem.* **2001**, *85*, 253–261.
[26] M. Casolaro, M. Chelli, M. Ginanneschi, F. Laschi, M. Muniz-Miranda, A. M. Papini, G. Sbrana, *Spectrochim. Acta Part A* **1999**, *55*, 1675–1689; L. Szyrwiel, J. S. Pap, L. Szczukowski, Z. Kerner, J. Brasun, B. Setner, Z. Szewczuk, W. Malinka, *RSC Adv.* **2015**, *5*, 56922–56931.
[27] C. Harford, B. Sarkar, *Acc. Chem. Res.* **1997**, *30*, 123–130.
[28] M. Blaszak, E. Jankowska, T. Kowalik-Jankowska, *Polyhedron* **2014**, *68*, 379–389.
[29] T. G. Fawcett, E. E. Bernarducci, K. Kroghjespersen, H. J. Schugar, *J. Am. Chem. Soc.* **1980**, *102*, 2598–2604.
[30] T. Kowalik-Jankowska, J. Jezierska, M. Kuczer, *Dalton Trans.* **2010**, *39*, 4117–4125.
[31] P. Mlynarz, D. Valensin, H. Kozlowski, T. Kowalik-Jankowska, J. Otlewski, G. Valensin, N. Gaggelli, *J. Chem. Soc. Dalton Trans.* **2001**, 645–652.
[32] P. L. T. Canh-Vang, A. Garnier, *Bioinorg. Chem.* **1978**, *8*, 21–31.
[33] M. R. Jensen, M. A. S. Hass, D. F. Hansen, J. J. Led, *Cell. Mol. Life Sci.* **2007**, *64*, 1085–1104.
[34] E. Gaggelli, N. D'Amelio, D. Valensin, G. Valensin, *Magn. Reson. Chem.* **2003**, *41*, 877–883.
[35] J. S. Pap, B. Kripli, V. Banyai, M. Giorgi, L. Korecz, T. Gajda, D. Arus, J. Kaizer, G. Speier, *Inorg. Chim. Acta* **2011**, *376*, 158–169.
[36] J. Peisach, W. E. Blumberg, *Arch. Biochem. Biophys.* **1974**, *165*, 691–708.
[37] J. I. Zink, R. S. Drago, *J. Am. Chem. Soc.* **1972**, *94*, 4550–4554.
[38] A. Matera, J. Brasun, M. Cebrat, J. Swiatek-Kozowska, *Polyhedron* **2008**, *27*, 1539–1555; T. Kowalik-Jankowska, M. Jasionowski, L. Lankiewicz, *J. Inorg. Biochem.* **1999**, *76*, 63–70.
[39] C. D. Geddes, *Meas. Sci. Technol.* **2001**, *12*, R53–R88.
[40] J. R. Lakowicz, *Principles of Fluorescence Spectroscopy*, Kluwer Academic/Plenum Publishers, New York, **1999**, pp. 1–24.
[41] V. Tõugu, A. Karafin, P. Palumaa, *J. Neurochem.* **2008**, *104*, 1249–1259.
[42] P. Cudic, M. Zinic, V. Tomisic, V. Simeon, J. P. Vigneron, J. M. Lehn, *J. Chem. Soc. Chem. Commun.* **1995**, 1073–1075.

[43] M. Sokolowska, W. Bal, *J. Inorg. Biochem.* **2005**, *99*, 1653 – 1660.
[44] B. Alies, E. Renaglia, M. Rozga, W. Bal, P. Faller, C. Hureau, *Anal. Chem.* **2013**, *85*, 1501 – 1508; R. de Ricco, D. Valensin, S. Dell'Acqua, L. Casella, C. Hureau, P. Faller, *ChemBioChem* **2015**, *16*, 2319 – 2328.
[45] R. F. Abdelhamid, Y. Obara, Y. Uchida, T. Kohzuma, D. M. Dooley, D. E. Brown, H. Hori, *J. Biol. Inorg. Chem.* **2007**, *12*, 165 – 173.
[46] W. Kim, Y. Kim, J. Min, D. J. Kim, Y. T. Chang, M. H. Hecht, *ACS Chem. Biol.* **2006**, *1*, 461 – 469.
[47] H. Levine, *Protein Sci.* **2008**, *2*, 404 – 410.
[48] H. Naiki, F. Gejyo, *Methods Enzymol.* **1999**, *309*, 305 – 318; C. L. Ni, H. P. Shi, H. M. Yu, Y. C. Chang, Y. R. Chen, *FASEB J.* **2011**, *25*, 1390 – 1401.
[49] K. C. Evans, E. P. Berger, C. G. Cho, K. H. Weisgraber, P. T. Lansbury, *Proc. Natl. Acad. Sci. USA* **1995**, *92*, 763 – 767; P. Hortschansky, V. Schroeckh, T. Christopeit, G. Zandomeneghi, M. Fandrich, *Protein Sci.* **2005**, *14*, 1753 – 1759; L. Nielsen, R. Khurana, A. Coats, S. Frokjaer, J. Brange, S. Vyas, V. N. Uversky, A. L. Fink, *Biochemistry* **2001**, *40*, 6036 – 6046.
[50] M. Mold, L. Ouro-Gnao, B. M. Wieckowski, C. Exley, *Sci. Rep.* **2013**, *3*, 1256.
[51] A. K. Sharma, S. T. Pavlova, J. Kim, L. M. Mirica, *Metallomics* **2013**, *5*, 1529 – 1536.
[52] C. J. Sarell, S. R. Wilkinson, J. H. Viles, *J. Biol. Chem.* **2010**, *285*, 41533 – 41540; X. D. Huang, C. S. Atwood, R. D. Moir, M. A. Hartshorn, R. E. Tanzi, A. I. Bush, *J. Biol. Inorg. Chem.* **2004**, *9*, 954 – 960.
[53] L. Guilloreau, S. Combalbert, A. Sournia-Saquet, H. Mazarguil, P. Faller, *ChemBioChem* **2007**, *8*, 1317 – 1325.
[54] M. A. Greenough, J. Camakaris, A. I. Bush, *Neurochem. Int.* **2013**, *62*, 540 – 555.
[55] R. A. Cherny, C. S. Atwood, M. E. Xilinas, D. N. Gray, W. D. Jones, C. A. McLean, K. J. Barnham, I. Volitakis, F. W. Fraser, Y. S. Kim, X. D. Huang, L. E. Goldstein, R. D. Moir, J. T. Lim, K. Beyreuther, H. Zheng, R. E. Tanzi, C. L. Masters, A. I. Bush, *Neuron* **2001**, *30*, 665 – 676.
[56] N. M. Chiera, M. Rowinska-Zyrek, R. Wieczorek, R. Guerrini, D. Witkowska, M. Remelli, H. Kozlowski, *Metallomics* **2013**, *5*, 214 – 221.
[57] A. R. Katritzky, T. Narindoshvili, P. Angrish, *Synthesis* **2008**, 2013 – 2022.
[58] E. Kaiser, R. Colescot, C. Bossinge, P. I. Cook, *Anal. Biochem.* **1970**, *34*, 595 – 598.
[59] H. Edelhoch, *Biochemistry* **1967**, *6*, 1948 – 1954.
[60] E. García-Fruitós, N. Gonzalez-Montalban, M. Morell, A. Vera, R. M. Ferraz, A. Aris, S. Ventura, A. Villaverde, *Microb. Cell Fact.* **2005**, *4*, 27.
[61] M. Carrió, N. Gonzalez-Montalban, A. Vera, A. Villaverde, S. Ventura, *J. Mol. Biol.* **2005**, *347*, 1025 – 1037.
[62] A. Villar-Piqué, A. Espargaro, R. Sabate, N. S. de Groot, S. Ventura, *Microb. Cell Fact.* **2012**, *11*, 55.

Received: January 21, 2016
Published online on April 13, 2016